Local mechanical properties of polymeric nanocomposites

George J. Papakonstantopoulos, Kenji Yoshimoto, Manolis Doxastakis, Paul F. Nealey, and Juan J. de Pablo*
Department of Chemical and Biological Engineering, University of Wisconsin-Madison, Madison, Wisconsin 53706-1691, USA
(Received 14 December 2004; revised manuscript received 27 May 2005; published 1 September 2005)

The inclusion of a nanoparticle into a polymer matrix is studied by efficient Monte Carlo simulations. The resulting structural changes in the melt and glass exhibit a strong dependence on the strength of the polymer attraction to the surface of the filler. The mechanical properties of the nanocomposite are analyzed in detail through a formalism that permits calculation of local elastic constants. The average shear and Young's modulus of the nanocomposite are higher than those of the pure polymer for neutral or attractive nanoparticles. For repulsive particles, these moduli are lower. Simulation of local properties reveals that a glassy layer is formed in the vicinity of the attractive filler, contributing to the increased strength of the composite material. In contrast, a region of negative moduli emerges around repulsive fillers, which provides a mechanism for frustration relief and a lowering of the glass transition temperature.

DOI: 10.1103/PhysRevE.72.031801 PACS number(s): 61.41.+e, 62.20.Dc, 62.25.+g, 81.05.Ni

I. INTRODUCTION

A considerable body of experimental work has shown that nanoparticle-reinforced polymeric materials can exhibit mechanical properties superior to those of the pure polymer [1,2]. That work has also shown that nanometer-scale particles are much more effective at reinforcing polymers than larger, micron-scale particles. The glass transition temperature (T_g) of a polymer nanocomposite can be higher or lower [2] than that of the pure polymer, depending on the nature of the nanoparticle-polymer interactions. Similarly, the elastic moduli of polymer nanocomposites can be higher or lower than those of the pure polymer [2]. In general, the mechanical attributes of a nanocomposite are not a simple average of the properties of the polymer and filler particles. Furthermore, significant changes are observed even for small-volume fractions ϕ of the filler, suggesting that the nature of any reinforcement (or weakening) is highly cooperative.

Considerable effort has been devoted to the theoretical and numerical study of polymer melts near flat, rigid walls [3]. Much less work, however, has been devoted to molecular-level theoretical or numerical studies of polymer reinforcement by nanometer scale particles. Furthermore, available studies have been limited to investigations of the structure of the polymer matrix in the presence of a small particle [4]. In the few cases where rheological or elastic properties have been considered [5], the aim has been to determine whether the average properties (viscosity and bulk modulus) of the composite are different from those of the pure polymer. It is generally accepted that a nanoparticle will perturb the conformation of the polymer around it. The question that arises then is whether such conformational changes are directly responsible for the mechanical behavior of the polymer; are any reinforcement or weakening effects of a polymer by nanometer-scale particles localized, and if so, what is the extent and magnitude of that localization?

II. METHODOLOGY

A. Simulations

The polymer molecules considered in this work consist of segments that interact with each other with a 12-6 Lennard-Jones (LJ) truncated potential, shifted at the cutoff $r_c=2.5\sigma$:

$$U_{nb}(r)=\begin{cases}4\varepsilon\left[\left(\frac{\sigma}{r}\right)^{12}-\left(\frac{\sigma}{r}\right)^{6}\right]-U_{LJ}(r_c), & r\leqslant r_c,\\ 0, & r>r_c,\end{cases} \quad (1)$$

where ε and σ are the Lennard-Jones parameters for the energy and length, respectively, and r the distance between the segments. The bonding energy between consecutive segments in the same chain is given by

$$U_b(r)=\frac{1}{2}k(r-\sigma)^2, \quad (2)$$

with bond constant $k=10^3\varepsilon/\sigma^2$. A literature model for colloidal suspensions is used to describe nanoparticle-polymer interactions [4]. It includes a 12-6 LJ potential, where distances are calculated from the surface of the particle of radius $R_f=2.0\sigma$:

*Author to whom all correspondence should be addressed. Electronic address: depablo@engr.wisc.edu

$$U_{nb}^{f}(r) = \begin{cases} 4\varepsilon_f\left[\left(\frac{\sigma_f}{r-R_f}\right)^{12} - \left(\frac{\sigma_f}{r-R_f}\right)^{6}\right] - U_{LJ}(r_c), & r-R_f \leqslant r_c, \\ 0, & r-R_f > r_c. \end{cases}$$

Three types of interactions are considered: strongly "attractive" ($\varepsilon_f=10\varepsilon$ and $r_c=2.5\sigma$), "neutral" ($\varepsilon_f=\varepsilon$ and $r_c=2.5\sigma$), and "repulsive" ($\varepsilon_f=\varepsilon$ and $r_c=2^{1/6}\sigma$). All systems consist of 450 chains of $N=32$ segments each. They are originally equilibrated at a dimensionless temperature of $T^*=1.2k_BT/\varepsilon$, with simulations in the *NPT* statistical ensemble. The temperature is then decreased gradually, allowing for sufficient equilibration of the system in between each step until a temperature of 0.2 is reached. All simulations are performed at a constant pressure $P^*=0.3\varepsilon/\sigma^3$. In the rest of the paper all quantities are reported in LJ reduced units. All simulations are run for at least 9×10^4 Monte Carlo (MC) cycles. A MC cycle consists of 3×10^4 trial moves. Polymer configurations are sampled by resorting to advanced MC trial moves that have been shown to circumvent many of the bottlenecks that are typically associated with simulation of long polymeric molecules at elevated densities. The use of these moves is essential to generate relevant, statistically significant configurations of the polymer around a nanoparticle. Individual monomers and the particle are displaced by random local movements and configurational-bias reptation moves. Internal rebridging (IB) and double rebridging (DB) trial moves are also implemented [6]. The latter trial moves involve the simultaneous exchange of parts of two neighboring chains and accelerate considerably the structural rearrangement of polymer molecules around a nanoparticle. The maximum distance for the random displacement moves was chosen in each temperature so that an acceptance ratio around 30% was achieved. The acceptance for the rebridging moves decreases when moving to lower temperatures, so fewer beads are chosen to be removed and reconstructed. Four beads or three beads are chosen for (IB) and (DB), respectively, at $T=1.2$, whereas two beads or one bead are used at $T=0.5$. In Table I a typical pattern of attempted trial moves is given for two temperatures, $T=0.3$ and 0.5, for a system with a neutral particle.

B. Formula for mechanical properties

The elastic moduli of the model composites considered in this work are calculated by measuring the thermal fluctuations of the local internal stress:

$$\sigma_{ij}^{m} = \rho^m k_B T\delta_{ij} - \frac{1}{l^3}\sum_{a<b}\left(\frac{\partial U}{\partial r^{ab}}\right)\frac{r_i^{ab}r_j^{ab}}{r^{ab}}\frac{q^{ab}}{r^{ab}}, \tag{3}$$

where ρ^m, k_B, T, and δ_{ij} are the number density of cube m, Boltzmann's constant, the temperature of the system, and the Kronecker delta, respectively. Subscripts denote Cartesian coordinates, U is the pairwise additive potential energy function, and r^{ab} is the distance between two interactions sites a and b. If the vector joining a and b, r_i^{ab}, passes through the cube m, the part of the line segment that lies inside the cube is defined by the variable q^{ab}. If the vector does not pass through the cube, then $q^{ab}=0$. Integration of σ_{ij}^m over the entire volume gives the internal stress tensor of the bulk system.

Following Yoshimoto *et al.* [1], the local mechanical properties of the system are determined by discretizing the simulation cell into small cubic elements. The local elastic modulus tensor C_{ijkl}^m is related to the internal stress fluctuations through the second derivative of the free energy with respect to the strain [7]:

$$C_{ijkl}^{m} = C_{ijkl}^{Bm} - C_{ijkl}^{Sm} + C_{ijkl}^{Km}, \tag{4}$$

where

$$C_{ijkl}^{Bm} = \frac{1}{l^3}\left\langle \sum_{\alpha<\beta}\left(\frac{\partial^2 U}{\partial r^{ab2}} - \frac{1}{r^{ab}}\frac{\partial U}{\partial r^{ab}}\right)\frac{r_i^{ab}r_j^{ab}r_k^{ab}r_l^{ab}}{r^{ab2}}\frac{q^{ab}}{r^{ab}}\right\rangle, \tag{5}$$

$$C_{ijkl}^{Sm} = \frac{V}{k_BT}[\langle\sigma_{ij}^m\sigma_{kl}\rangle - \langle\sigma_{ij}^m\rangle\langle\sigma_{kl}\rangle], \tag{6}$$

TABLE I. Typical pattern of attempts of moves and acceptance for $T=0.3$ and 0.5 for a system with a neutral particle.

T	0.3		0.5	
Type of move	% trial moves	% accepted	% trial moves	% accepted
Random displacement	79.5	30.0	55.0	30.0
Particle displacement	0.5	30.0	0.5	30.0
Reptation	10.0	3×10^{-3}	19.5	6×10^{-3}
Internal rebridging	10.0	0.3	20.0	0.6
Double rebridging	0.0	—	5.0	2×10^{-3}

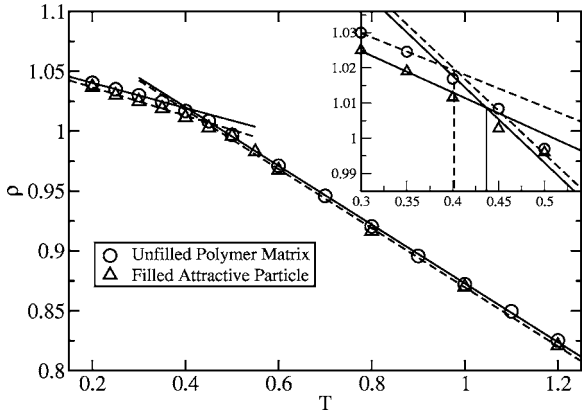

FIG. 1. Density of the polymer matrix (substracting the volume of the particle) over a wide temperature range for the unfilled and attractive filler case. For clarity, results for other type of interactions are not shown. The glass transition temperature is extracted from the change of the slope. In the inset, the same results are presented but magnified for the range of interest. The lines are linear regressions of the data (solid line, unfilled polymer; dashed line, attractive particle).

$$C_{ijkl}^{Km} = 2\langle \rho^m \rangle k_B T(\delta_{ij}\delta_{kl} + \delta_{ik}\delta_{jl}). \tag{7}$$

We point out that the Born term C_{ijkl}^{Bm} represents the instantaneous elastic modulus for any given configuration subject to a uniform infinitesimal strain. The contribution of the kinetic term is denoted by C_{ijkl}^{Km}. The stress fluctuation term C_{ijkl}^{Sm} accounts for the "internal particle motions" that arise from thermal fluctuations.

III. RESULTS AND DISCUSSION

Consistent with results of previous simulations of polymers near walls or particles, the density profile of the monomers around the particle exhibits pronounced oscillations [3–5]. Our simulations also show an enhancement of chain ends near the surface of the particles for neutral and repulsive interactions and a depletion for attractive systems. In general, it is observed that polymer segments align parallel to the surface of the particle. The orientation of segments for all three cases studied here is essentially the same. These results are consistent with other off-lattice simulations that have verified the tendency of segments to lie parallel to the surface for both wall [3] and spherical particle [4,5] cases. Calculations of the chain gyration tensor **S** indicate that in vicinity of the particle the chains are "flattened" in the directions parallel to the surface and they are shrunk in the direction normal to it. The effect of the surface on the chain shape is relatively short ranged. Similar observations have been reported before for chains near a wall [3] or near a particle [4]. These structural results serve to emphasize that the behavior of the model considered in this paper is consistent with that of other, different models considered in the literature for study of nanocomposites.

The glass transition temperature can be estimated by plotting the density with respect to temperature (Fig. 1). The temperature where the slope of the density curve changes can be associated to the glass transition temperature. The glass transition temperature of the pure, unfilled polymer matrix is $T_g^{pol}=0.4$ [8]. The filled nanocomposite systems exhibit a shift of T_g; for a repulsive particle, the shift is negative and $T_g^{rep}=0.38$. For the neutral and attractive particles, we find $T_g^{neut}=0.41$ and $T_g^{attr}=0.43$, respectively.

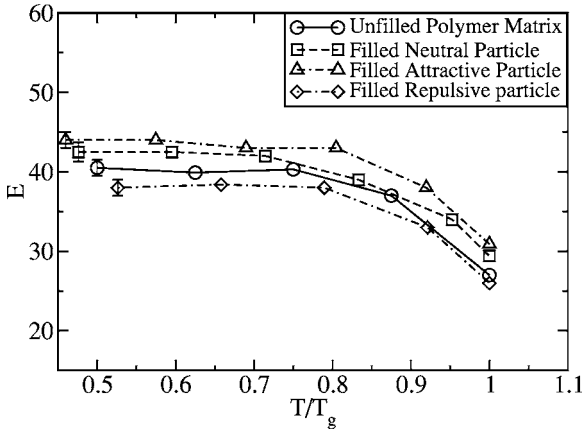

FIG. 2. Young's modulus E as a function of temperature divided by the glass transition temperature of each system for all cases studied in this paper.

Figure 2 shows Young's modulus E as a function of temperature for the three particles considered in this study. E is calculated from the components of the elasticity tensor as

$$E = \frac{\bar{C}_{44}(3\bar{C}_{12} + 2\bar{C}_{44})}{\bar{C}_{12} + \bar{C}_{44}}, \tag{8}$$

where $\bar{C}_{12}=(C_{12}+C_{13}+C_{23})/3$ and $\bar{C}_{44}=(C_{44}+C_{55}+C_{66})/3$ ($\bar{C}_{44}$ is the shear modulus). Below T_g, the Young's modulus of the nanocomposite system for the neutral and attractive case is higher than that of the pure polymer. For the repulsive particle, however, the modulus is lower. This observation is consistent with results of experiments [2]. The glass transition temperatures inferred from the drop of E are consistent with those obtained from curves of the density as a function of temperature.

It is important to emphasize that the changes reported in Fig. 2 for the Young's modulus are a reflection of structural changes of the polymer matrix; the particle itself is rigid, and it only contributes to elastic moduli through the polymer-particle interactions. The modulus changes observed in this work are consistent with the viscosity changes reported by Smith *et al.* [5] in the melt regime (above T_g). Attractive and neutral particles were found to increase the viscosity of the polymer, while repulsive particles were found to reduce it. Brown *et al.* [5] have also reported that, for repulsive interactions between the particle and polymer matrix, the inverse compressibility (or bulk modulus) of the composite is lower than that of the pure polymer. Those simulations, however, considered only the compressibility of an individual polymer molecule interacting with itself through periodic boundary conditions; it is unclear how a many-chain system would behave. In different work, using a lattice model and an ap-

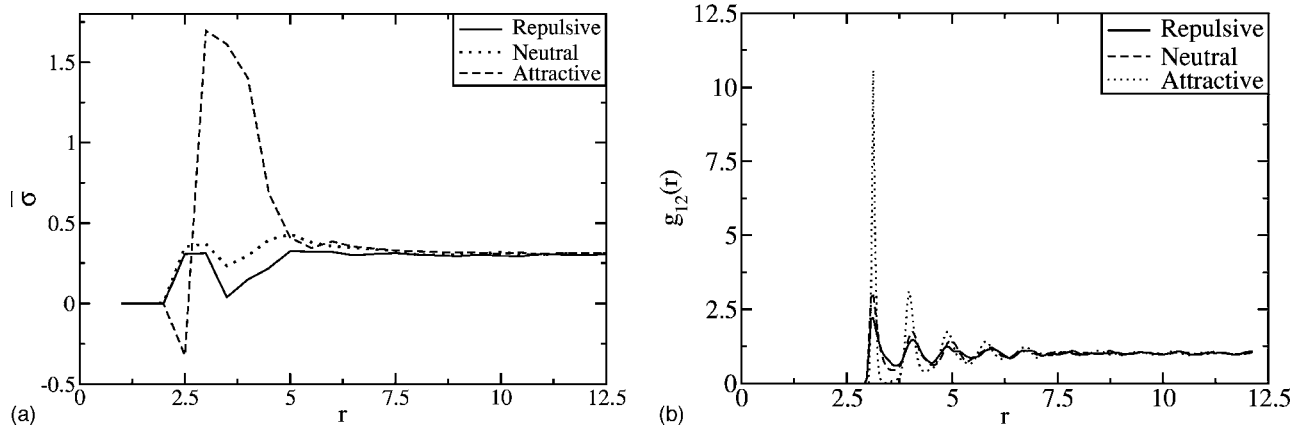

FIG. 3. (a) Distribution of the local stress $\bar{\sigma}$ with respect to the distance r from the center of the nanoparticle for the three types of interaction considered in this paper, at $T=0.5$. (b) Filler-monomer pair distribution function $g_{12}(r)$ for $T=0.5$ as a function of the distance r from the center of the nanoparticle.

proximate treatment of polymer conformations, Sharaf and Mark [5] have reported an increase of the modulus of nanocomposites above that of the pure polymer. Note, however, that local packing effects play a dominant role in the mechanical behavior of nanocomposites, and it is not clear whether a lattice model can capture such effects or not.

Figure 3(a) shows the trace of the *local* stress tensor $\bar{\sigma}=(\sigma_{xx}+\sigma_{yy}+\sigma_{zz})/3$ as a function of distance from the center of the nanoparticle. For the attractive system, the stress in the immediate vicinity of the particle is negative, and then it is followed by a region of compression, where the stress is considerably larger and positive. As one moves away from the particle, the local stress becomes equal to the pressure of the system, showing that bulk behavior is recovered at a distance of approximately R_g ($R_g=2.89\pm0.03$). The region over which the local stress is different from the bulk corresponds to the region over which packing effects arising from the particles are felt (approximately $r\approx7.5$ from the center of the nanoparticle), as indicated by the oscillations of the radial distribution shown in Fig. 3(b). Simulations of polypropylene near a graphite wall [3] also show that the normal component of the stress is strongly compressive near the surface. The neutral and repulsive exhibit different characteristics. Moving away from the particle's surface, the stress profile oscillates and gradually increases to the bulk value of the pressure. In these two cases, however, there is a first peak followed by a stress well where the stress drops considerably, and then a second peak can be seen and finally a decrease to the bulk value. The average stress $\bar{\sigma}$ is higher for the neutral system than for the repulsive system, indicating that the molecules are more compressed near a neutral particle.

Figure 4(a) shows the *local* shear modulus as a function of the distance from the surface of the filler. An increase of the local $\bar{C}_{44}$ is observed for the attractive and neutral systems in the vicinity of the particle. This pronounced increase is indicative of the existence of a glassy layer around the particles, even at temperatures above the glass transition ($T/T_g=1.16$). Berriot *et al.* [2] have hypothesized that a high-modulus layer exists around nanoparticles to interpret their experimental T_g data. Our observations provide direct evidence in support of the existence of that layer.

The results for the neutral and repulsive system are particularly intriguing. The nanoparticle is surrounded by a region of negative modulus which is followed by a second

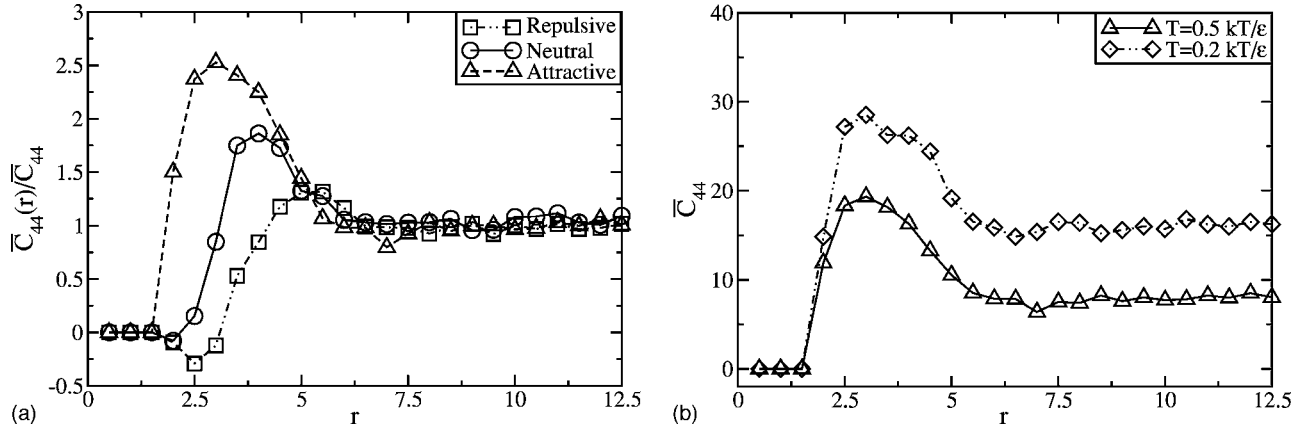

FIG. 4. (a) Distribution of the local $\bar{C}_{44}$ with respect to the distance r from the center of the nanoparticle for the three types of interaction considered at $T=0.5$. (b) Distribution of the local $\bar{C}_{44}$ with respect to the distance r from the center of the nanoparticle for the attractive particle in the melt and glass regime.

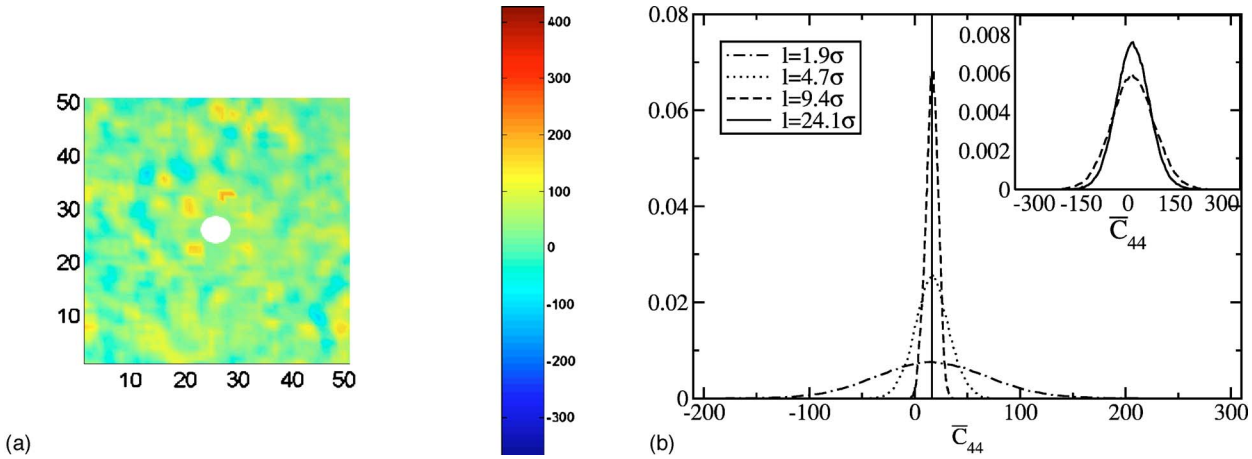

FIG. 5. (a) (Color online) Color map of the local shear modulus $\bar{C}_{44}$ around the attractive nanoparticle at $T=0.2$. (b) Distribution of the local $\bar{C}_{44}$ for different cube lengths at $T=0.2$. A Gaussian distribution is observed for all levels of resolution. The inset compares the distributions for the pure and the filled polymer at the highest level of resolution considered here, $l=1.9\sigma$.

region having a modulus higher than that of the bulk. These domains of negative and large positive moduli cannot be explained solely in terms of density. As Fig. 3(b) indicates, the density near the particle, in the region where the modulus is negative, is higher than away from the particle, where the modulus is higher than in the bulk.

Figure 4(b) shows the local shear modulus as a function of temperature for the attractive particle. It can be seen that, as the temperature decreases, the shear modulus of the solidlike layer around the particle increases. The thickness of that glassy layer also increases (with lower temperatures) and finally reaches a constant value at and below T_g. That thickness is approximately equal to 2.5σ and is comparable to the R_g of the polymer. Far from the particle, the shear modulus decays to the value corresponding to the pure polymer at that temperature. Figure 5(a) shows a color map of the local shear modulus of the nanocomposite. The figure reveals the existence of domains having a modulus that is considerably higher or lower than the average value. A preponderance of domains with a large, positive modulus is observed in the immediate vicinity of the nanoparticle. Contrary to our expectations, however, stiff domains are not arranged in well-defined "shells" around the nanoparticle, but adopt an appearance similar to that of domains in the bulk. Figure 5(b) shows the distribution of local shear moduli as a function of the level of resolution with which the local moduli are calculated. These distributions remain Gaussian down to the highest level of resolution considered in this work ($l=1.9\sigma$) (see Fig. 5). For $l=1.9\sigma$, there are approximately ten monomers per cubic element. It is found that, consistent with results for the pure polymer, domains of large negative modulus are stabilized by the existence of regions of high, positive modulus. We find that the distribution of local moduli for the nanocomposite is narrower [see inset of Fig. 5(b)] than it is for the pure polymer. This finding suggests that one of the mechanisms through which nanoparticles reinforce glassy polymers is by reducing the degree of mechanical inhomogeneity that arises at nanometer length scales. Less inhomogeneity would render the composite material not only stronger, but also more resistant to failure. Similarly, it is found that neutral or repulsive nanoparticles also decrease the mechanical heterogeneity of the polymer. Such particles, however, give rise to formation of negative stiffness layers around them. They reduce heterogeneity by relieving frustration in the system and result in a lower T_g.

IV. CONCLUSIONS

In summary, results of Monte Carlo simulations of polymer nanocomposites reveal that, even *above* the glass transition temperature, nanoparticles induce the formation of a solidlike, glassy layer. Such a layer is characterized by large, solidlike elastic moduli. The existence of this glassy layer, which has been invoked in the past to explain the experimentally observed increases of the storage modulus in nanocomposites, is confirmed directly through precise calculations of *local* mechanical properties. Below the glass transition temperature, the nanoparticles serve to reduce the degree of mechanical inhomogeneity that characterizes polymer glasses. A reduction of inhomogeneity helps explain why nanocomposite glasses are not only stronger, but also more resistant to failure.

ACKNOWLEDGMENTS

This work is supported by Chemical Sciences, Geosciences and Biosciences Division, Office of Basic Energy Sciences, Office of Science, U.S. Department of Energy (DE-FG02–99ER14961). Partial support from the Semiconductor Research Corporation (SRC) is also gratefully acknowledged.

[1] K. Yoshimoto, T. S. Jain, K. Van Workum, P. F. Nealey, and J. J. de Pablo, Phys. Rev. Lett. **93**, 175501 (2004).

[2] B. Ash, R. Siegel, and L. Schadler, Macromolecules **37**, 1358 (2004); J. Berriot, H. Montes, F. Lequeux, D. Long, and P. Sotta, *ibid.* **35**, 9756 (2002); M. Kobayashi, Y. Rharbi, L. Brauge, L. Cao, and M. A. Winnik, *ibid.* **35**, 7387 (2002); Y. Ou, F. Yang, and Z. Yu, J. Polym. Sci., Part B: Polym. Phys. **36**, 789 (1998); P. Vollenberg and D. Heikens, Polymer **30**, 1656 (1989).

[3] C. Abrams and K. Kremer, J. Chem. Phys. **115**, 2776 (2001); I. Bitsanis and G. Hadziioannou, *ibid.* **92**, 3827 (1990); K. Mansfield and D. Theodorou, Macromolecules **24**, 4295 (1991); M. Steinfath and W. Bruns, Macromol. Theory Simul. **6**, 749 (1997).

[4] R. Picu and M. Ozmusul, J. Chem. Phys. **118**, 11239 (2003); P. Scheidler, W. Kob, and K. Binder, Europhys. Lett. **59**, 701 (2002); F. Starr, T. Schrøder, and S. Glotzer, Macromolecules **35**, 4481 (2002); M. Vacatello, *ibid.* **34**, 1946 (2001); M. Doxastakis, Y.-L. Chen, O. Guzmán, and J. de Pablo, J. Chem. Phys. **120**, 9335 (2004).

[5] D. Brown, P. Mélé, S. Marceau, and N. Alberola, Macromolecules **36**, 1395 (2003); M. Sharaf and J. Mark, Polymer **45**, 3943 (2004); G. Smith, D. Bedrov, L. Li, and O. Byutner, J. Chem. Phys. **117**, 9478 (2002).

[6] Z. Chen and F. Escobedo, J. Chem. Phys. **113**, 11382 (2000); B. Banaszak and J. de Pablo, *ibid.* **119**, 2456 (2003); N. C. Karayiannis, V. G. Mavrantzas, and D. N. Theodorou, Phys. Rev. Lett. **88**, 105503 (2002).

[7] J. Lutsko, J. Appl. Phys. **64**, 1152 (1988).

[8] T. S. Jain and J. J. dePablo, Phys. Rev. Lett. **92**, 155505 (2004).